Supplementary Data

Kinematics of an OSPA actuator composed of a series of modules

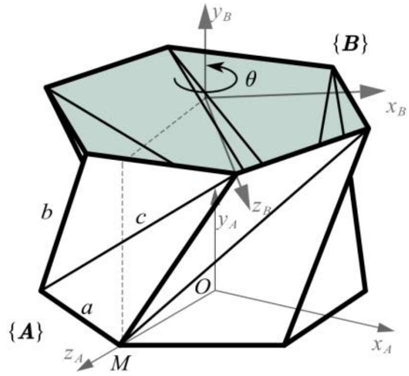

SUPPLEMENTARY FIG. S1 Coordinate system of the kinematics model of twisting motion.

From elemental rotation matrix of *y*-axis, we have,

$$R_y = \begin{bmatrix} \cos\ \theta & 0 & \sin\ \theta \\ 0 & 1 & 0 \\ -\sin\ \theta & 0 & \cos\ \theta \end{bmatrix}, \tag{S1}$$

where θ represents relative rotation angle as shown in Fig. 2(A). There is a homogeneous transformation matrix H which contains relative position and attitude information between the two coordinate systems $\{\boldsymbol{A}\}$ and $\{\boldsymbol{B}\}$,

$$H = \begin{bmatrix} R_y & {}^{A}p_{ab} \\ 0 & 1 \end{bmatrix}, \tag{S2}$$

where ${}^{A}p_{ab}$ is the position vector from $\{\boldsymbol{B}\}$ to $\{\boldsymbol{A}\}$, and ${}^{A}R_B$ refers to the rotational transformation matrix which describes the pose of $\{\boldsymbol{B}\}$ with respect to $\{\boldsymbol{A}\}$. The rigid-body transformation of the top plate with respect to the and bottom plate is given by,

$$H = \begin{bmatrix} \cos\theta & 0 & \sin\theta & 0 \\ 0 & 1 & 0 & b - \dfrac{b}{60^\circ}|\theta| \\ -\sin\theta & 0 & \cos\theta & 0 \\ 0 & 0 & 0 & 1 \end{bmatrix}. \tag{S3}$$

The equation can also be written as,

$$H = \begin{bmatrix} R_y(\theta) & \left(b - \dfrac{b}{60^\circ}|\theta|\right)\vec{v} \\ \vec{0}^T & 1 \end{bmatrix} \in R^{4\times 4}, \tag{S4}$$

where $\vec{v} = [0 \quad 1 \quad 0]^T$.

For the OSPAs with n modules, the transformation matrix from the first OSPA module to the end is,

$$^{0}H_{n}=\begin{bmatrix}\prod_{i=1}^{n}R_{y}(\theta_{i}) & \left(nb-\frac{b}{60^{\circ}}\sum_{i=1}^{n}|\theta_{i}|\right)\vec{v}\\ \vec{0}^{T} & 1\end{bmatrix}\in R^{4\times4}, \quad \text{(S5)}$$

where for Actuator IB there is $b=2a$, $h=2\text{a}\cdot\sin\left(\frac{\theta}{2}\right)$. Using these equations, we can analyze the kinematics of an OSPA actuator composed of a series of modules.

Flexural rigidity and elastic constants

Referring to Silverberg's test method mentioned in the supplementary material[36], several creases 1 mm in length and width were modeled in silicone E615 with two different thicknesses: 1.2 mm and 0.6 mm in FEA simulation. The creases were bent by 60° and the torque was linearly proportional to the bending angular deflection by a constant k_c . When the thickness of crease is 1.2 mm, $k_{c1}=2\ N/rad\simeq3.49\times10^{-2}\ N/^{\circ}$ and $k_{c2}=0.25\ N/rad\simeq4.36\times10^{-3}\ N/^{\circ}$ for thickness of 0.6 mm.

Volume of the OSPA module and the rotation angle of the folds

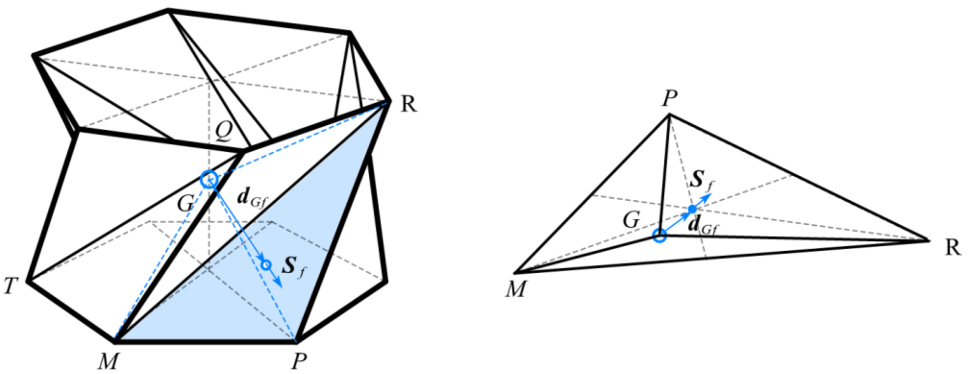

SUPPLEMENTARY FIG. S2 The sub-element pyramid G-MPR from OSPA module.

Volume of the tetrahedron formed by the geometric center G and the plane MPR can be given as,

$$V_{pyramid}=\frac{1}{3}\boldsymbol{d}_{Gf}\cdot\boldsymbol{S}_{f}, \quad \text{(S6)}$$

where $\boldsymbol{d}_{Gf}$ is the vector from geometric center G to the center of the polygon f and $\boldsymbol{S}_{f}$ is the normal vector of plane MPR.

In Fig. 2(A), the coordinates of the four points MQPR and geometric center G on truss structure can be written as,

$$\begin{cases} M(0,0,a) \\ P\left(\frac{\sqrt{3}}{2}a, 0, \frac{a}{2}\right) \\ Q(a \cdot \sin\theta_u, h, a \cdot \cos\theta_u) \\ R(a \cdot \sin(\theta_u + 60°), h, a \cdot \cos(\theta_u + 60°)) \\ G\left(0, \frac{h}{2}, 0\right) \end{cases} . \tag{S7}$$

In this way, the relationship between the volume of the OSPA module and θ_u can be given as,

$$\begin{aligned} V_C(\theta_u) &= 12 \cdot V_{GRMP} + 2 \cdot \left(\frac{1}{3} \cdot \frac{h}{2} \cdot S_{bottom}\right) \\ &= 4 \cdot (\text{proj}_{s_f} \boldsymbol{GP}) \cdot S_{MPR} + \frac{h}{3} \cdot S_{bottom} \\ &= \frac{\sqrt{2}\, a^2\, b\, \left(2\,\sigma_1 + \sqrt{3}\right) \sigma_2 \sqrt{4\,|\sigma_3|\, |a\, b\, \sigma_1|^2 + 4\,|\sigma_3|\, |a\, b\, \sin(\theta_u + 30^\circ)|^2 + |a|^4\, |b|^2\, \left|2\,\sigma_1 - \sqrt{3}\right|^2}}{4\,|b| \sqrt{a^4 \cos(\theta_u)^2 - 2\,a^4 + 2\,a^2\,b^2 + a^4\cos(\theta_u) + \sqrt{3}\,a^4 \sin(\theta_u) - \sqrt{3}\,a^4 \cos(\theta_u)\sin(\theta_u)}} \\ &\quad + \frac{\sqrt{3}\, a^2\, \bar{\sigma}_2\, \bar{b}}{2} \end{aligned}$$

$$, \tag{S8}$$

where $\sigma_1 = \cos(\theta_u + 30^\circ)$, $\sigma_2 = \sqrt{\frac{\sigma_3}{b^2}}$, $\sigma_3 = b^2 - 2\,a^2 + 2\,a^2 \cos(\theta_u)$ and S_{bottom} represent the area of the hexagon base.

The rotation angles of the folds QR, QM, RM can be written as,

$$\theta_{QM} = \arccos\left(\frac{|(\boldsymbol{QM} \times \boldsymbol{QR}) \cdot (\boldsymbol{QM} \times \boldsymbol{MT})|}{|\boldsymbol{QM} \times \boldsymbol{QR}| \cdot |\boldsymbol{QM} \times \boldsymbol{MT}|}\right), \tag{S9}$$

$$\theta_{QR} = \arccos\left(\frac{|(\boldsymbol{QM} \times \boldsymbol{QR}) \cdot (\boldsymbol{n}_s)|}{|\boldsymbol{QM} \times \boldsymbol{QR}| \cdot |\boldsymbol{n}_s|}\right), \tag{S10}$$

$$\theta_{RM} = \arccos\left(\frac{|(\boldsymbol{QM} \times \boldsymbol{QR}) \cdot (\boldsymbol{RM} \times \boldsymbol{MP})|}{|\boldsymbol{QM} \times \boldsymbol{QR}| \cdot |\boldsymbol{RM} \times \boldsymbol{MP}|}\right), \tag{S11}$$

where $\boldsymbol{n}_s = [0, 1, 0]$.

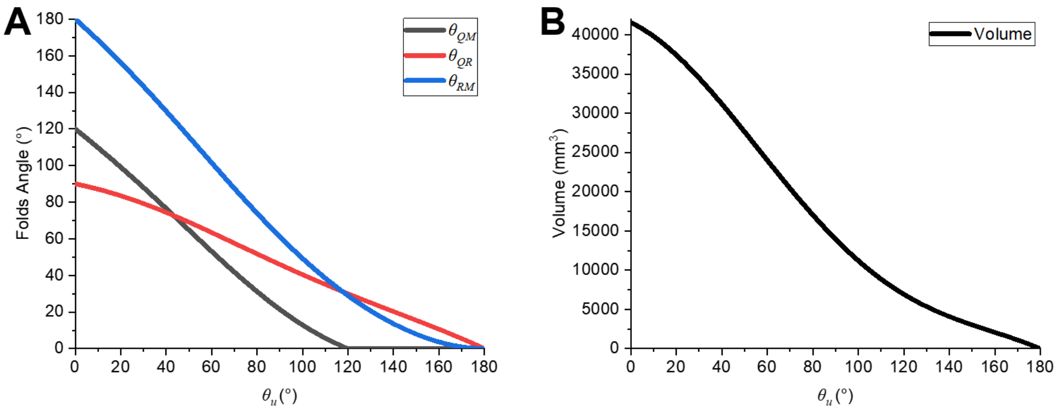

SUPPLEMENTARY FIG. S3 (A) The rotation angles of the folds QM, QR, RM are plotted as a function of relative rotation angle θ_u. (B) Volume of the OSPA module (V_C) is plotted as a function of relative rotation angle θ_u.

SUPPLEMENTARY Table S1 Fitting results

Material	Parameters
Ecoflex 00-30	$C_{10} = 0.00364188$ $C_{20} = 0.000573251$ $C_{30} = -3.93058e-06$
E615	$C_{10} = 0.0727207$ $C_{20} = 0.00527073$ $C_{30} = -7.73102-05$
Mixture（Dragonskin 30: Ecoflex 00-30=1:1）	$C_{10} = 0.0683405$ $C_{20} = 0.00958809$ $C_{30} = -0.000363852$

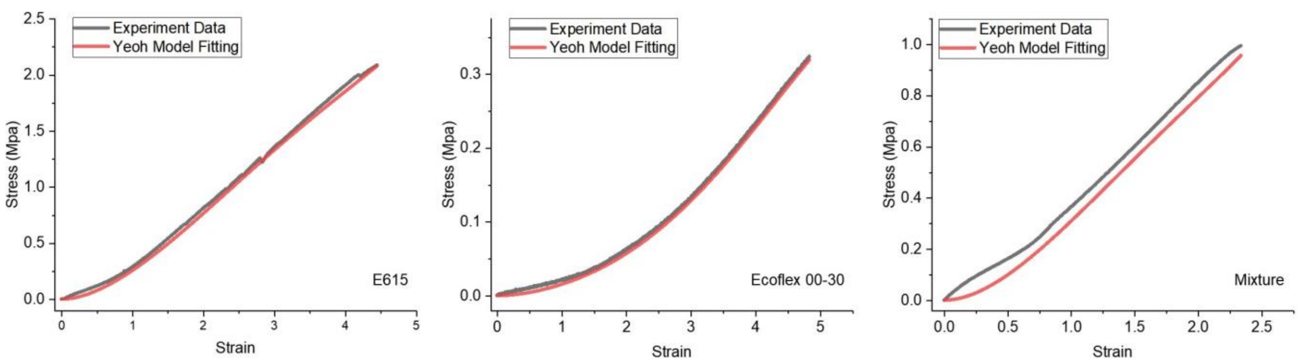

SUPPLEMENTARY FIG. S4 Stress-strain curves of three materials. (A) E615 From Hongyejie Inc. (B) Ecoflex 00-30 from Smooth-on. (C) The mixed components of Dragonskin 00-30 and Ecoflex 00-30 with a 1:1 weight ratio. Uniaxial tensile tests were performed more than five times for each material, using the tensile testing machine from MTS (Model 42). The standard throughout the whole experiment was referred to ASTM D412 rubber tensile test which is the most common standard for determining the tensile properties of (silicone) rubber. Dimensions of testing specimens are as defined in Type C of D412.

SUPPLEMENTARY FIG. S5 Experimental setup for measuring stress-strain curves.

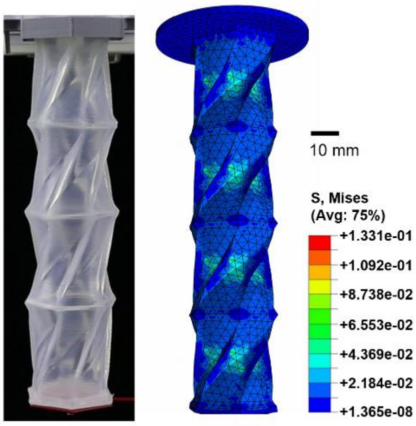

SUPPLEMENTARY FIG. S6 Actuator IB of E615 at a positive pressure of about 2 kPa in the experiment and the FEA simulation.

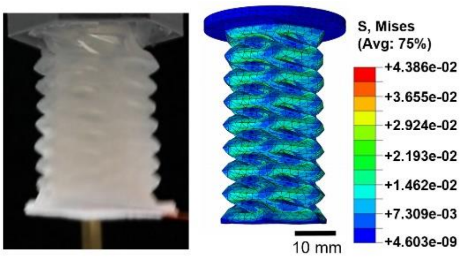

SUPPLEMENTARY FIG. S7 Actuator IA of E615 at a negative pressure about -3 kPa in the experiment and the FEA simulation.

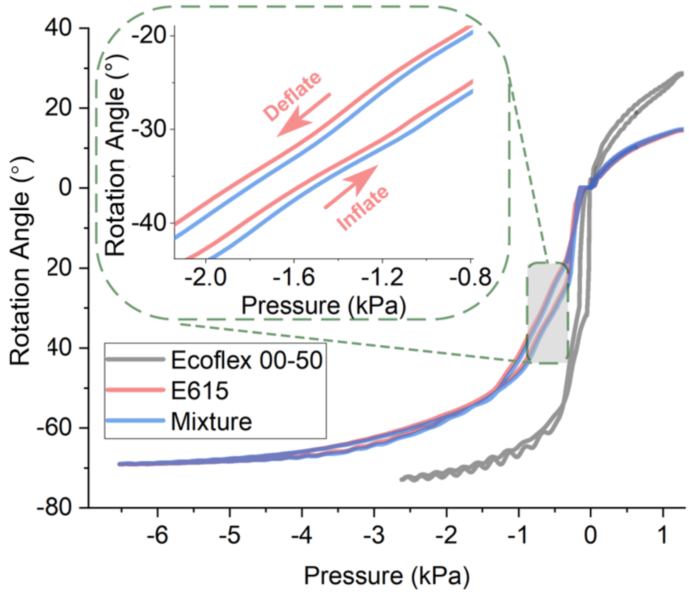

SUPPLEMENTARY FIG. S8 Simulation results of the variation of rotation angle with pressure for the module Type IB made of three different silicone.

SUPPLEMENTARY TABLE S2. Coating process of the OSPAs

Step	Tasks	Time	Note
1	Prepare the silicone precursor, weight ratio A:B=1:1 and stir with a coffee stick for 2-3 mins	5-8 mins	This step does not require vacuum defoaming
2	Evenly dip-coat the inside of the mold in sequence, fix the finished dip-coated mold to the inner frame of the spin-coater and turn on the spin-coating machine	20 mins	Dip coating for approx. 5 mins, and spin coating need to be at room temperature
3	Remove the mold from the spin coater and transfer it to the vacuum oven, close the balance valve and turn on the vacuum pump to defoam	~ 5 mins	
4	Turn off the vacuum pump and slowly unscrew the balance valve	5 mins	
5	After the previous step, the mold should be immediately transferred to a flat surface (e.g. a square Petri dish) and cured by heating (45°C) for 30 mins	30 mins	
6	Repeat steps 2-5, depending on the desired thickness, usually 3 times	—	The direction of the mold needs to be changed each time after it is dipped.
7	Evenly coat a piece of non-woven fabric slightly smaller than a square Petri dish with silica gel, place the mold on top of the silica gel, seal its	—	

	side, vacuum defoam and heat, and repeat steps 3-5	
8	Using the twist-off demolding method, peel the cured silicone from the mold, and insert the internal support skeleton from the other side (if it is needed)	—
9	Referring to step 7, seal the other side and heat to cure	30 mins
10	Takeout the cured product and check air tightness	—
11	Cut a small hole in the center of one side and use the connector to seal with silicone	30 mins-1 hour
12	Waiting for curing, finished	—

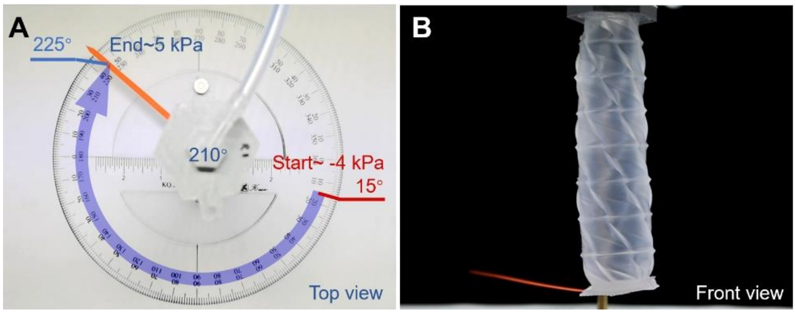

SUPPLEMENTARY FIG. S9 Experimental setup for measuring rotation angle (Actuator IA).

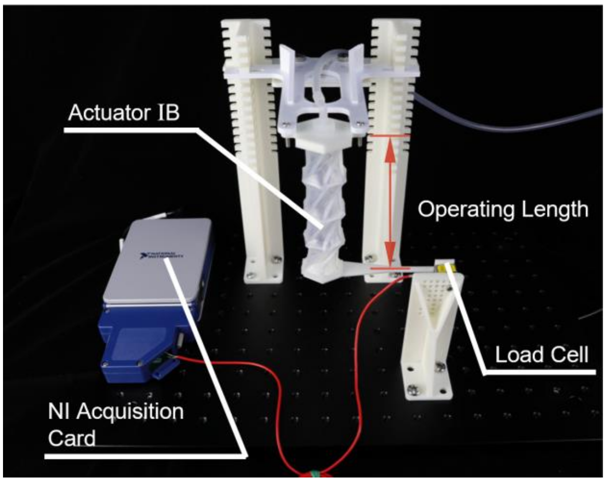

SUPPLEMENTARY FIG. S10 Experimental setup for torque testing (Actuator IB).

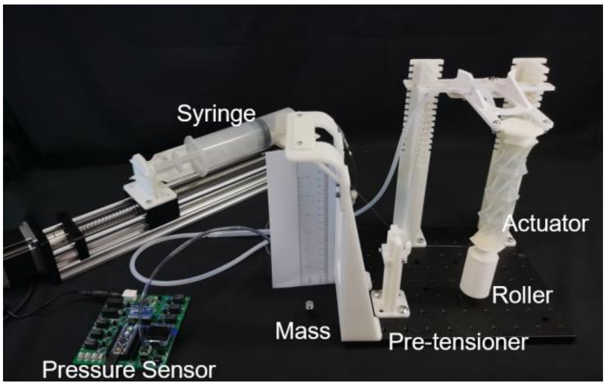

SUPPLEMENTARY FIG. S11 Experimental setup for life testing (Actuator IB).

OSPA's internal support skeleton

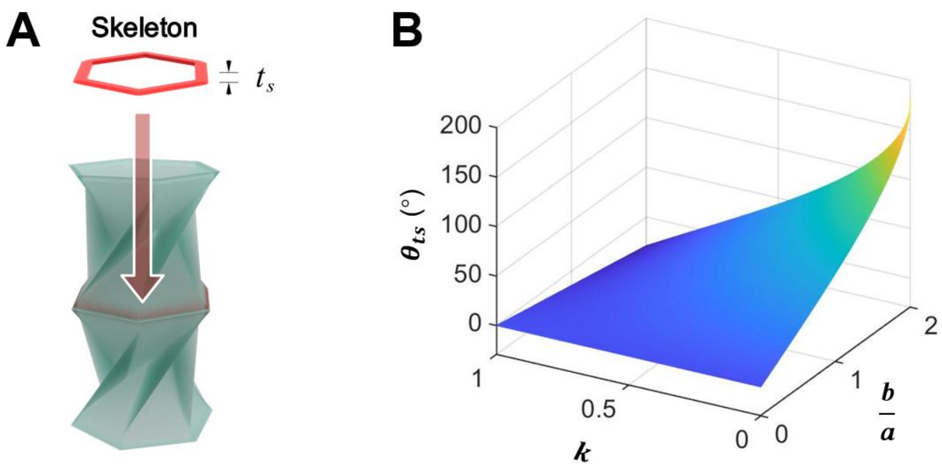

SUPPLEMENTARY FIG. S12 (A) OSPA's internal support skeleton. (B) The influence of k and b/a on the maximum rotation angle when the skeleton is inserted (θ_{ts}).

Occasionally, under extreme loads, the actuator may unfavorably collapse in the radial direction. To avoid this deformation and generate a larger load capacity, we insert internal skeletons made by Polylactic Acid (PLA) or Thermoplastic polyurethanes (TPU) to support the structure.

When the support structure is inserted, the thickness of the skeleton t_s influences the movement of the OSPA module. Assuming that the surface of the skeleton and the OSPA do not slide relative to each other during the actuation, we can obtain the following equation,

$$\theta_{ts} = 2\arcsin\left(\frac{b}{2a}\left(1-\frac{k}{\sin\delta_0}\right)\right), \tag{S12}$$

where t_s is the thickness of the skeleton and $k=\frac{t_s}{b}$. It can be seen that keeping the thickness of the support structure thin has only a modest effect on the maximum rotation angle. The thickness of the internal support skeleton we used is usually less than $b/20$, which minimizes the effect on the overall kinematics.

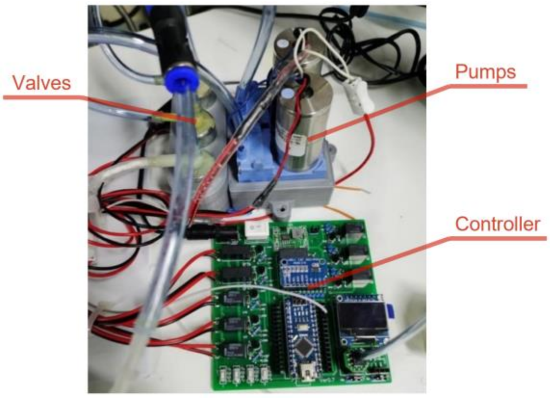

SUPPLEMENTARY FIG. S13 A pneumatic controller with two pumps and four valves. Self-designed pneumatic controller based on Arduino nano, up to three independent actuators can be driven simultaneously, with 16bit ADC sampling, air pressure monitoring and other functions.